



## Solvent-Free Composite PEO-Ceramic Fiber/Mat Electrolytes for Lithium Secondary Cells

Chunsheng Wang,<sup>a,\*</sup> Xiang-Wu Zhang,<sup>b,\*\*</sup> and A. John Appleby<sup>b,\*</sup>

<sup>a</sup>Center for Manufacturing Research and Department of Chemical Engineering, Tennessee Technological University, Cookeville, Tennessee 38505, USA

<sup>b</sup>Center for Electrochemical Systems and Hydrogen Research, Texas Engineering Experiment Station, Texas A&M University, College Station, Texas 77843-3402, USA

Solvent-free composite poly(ethylene oxide) (PEO)-ceramic fiber or mat electrolytes with high ionic conductivity and good interfacial stability have been developed using high-ionic-conductivity  $\text{La}_{0.55}\text{Li}_{0.35}\text{TiO}_3$  fibers and mats. The conducting ceramic fibers can penetrate the cross section of the electrolyte film to provide long-range lithium-ion transfer channels, thus producing composite electrolytes with high conductivity. In this work, a maximum room-temperature conductivity of  $5.0 \times 10^{-4} \text{ S cm}^{-1}$  was achieved for 20 wt %  $\text{La}_{0.55}\text{Li}_{0.35}\text{TiO}_3$  fiber in a PEO-LiN(SO<sub>2</sub>CF<sub>2</sub>CF<sub>3</sub>)<sub>2</sub> mixture containing 12.5 wt % Li<sup>+</sup> in PEO. The maximum transference number obtained was 0.7. The ceramic fibers in this composite electrolyte are coated by a very thin PEO layer, which is sufficient to provide good interfacial stability with lithium-ion and lithium-metal anodes.

© 2004 The Electrochemical Society. [DOI: 10.1149/1.1828952] All rights reserved.

Manuscript submitted May 17, 2004; revised manuscript received June 18, 2004. Available electronically December 6, 2004.

Solvent-free all-solid-state rechargeable lithium secondary cells have been studied extensively in recent years for cellular telephones, laptop computers, electric and hybrid vehicles, and aerospace applications. In a solid-state lithium cell, solid electrolytes serve both as ionic conductor and separator. Therefore, they must meet requirements of high ionic conductivity, high lithium ion transference number, a wide electrochemical stability window, easy processability, and acceptable thermal and mechanical properties. Electrolytes based on poly(ethylene oxide) (PEO) form dimensionally stable films and show high chemical stability to reduction, but have room-temperature conductivities that are too low ( $10^{-7}$  to  $10^{-8} \text{ S-cm}^{-1}$ ) for most applications. Certain ceramics and glasses show much higher Li-ion conductivity. Lithium lanthanum titanate ceramic ( $\text{La}_{0.55}\text{Li}_{0.35}\text{TiO}_3$ ) has the highest solid-state Li<sup>+</sup> conductivity reported to date ( $\sim 10^{-3} \text{ S-cm}^{-1}$ ) at room temperature.<sup>1-4</sup> Its conductivity of  $1.8 \times 10^{-5} \text{ S-cm}^{-1}$  at  $-50^\circ\text{C}$  is higher than that of typical PEO compositions at  $25^\circ\text{C}$ . Unfortunately,  $\text{La}_{0.55}\text{Li}_{0.35}\text{TiO}_3$  ceramic cannot be directly used in lithium secondary cells because it is chemically unstable below 1.5 V vs. Li<sup>0</sup> due to Ti(IV) to Ti(III) reduction.<sup>1,3</sup> To enhance the chemical stability of  $\text{La}_{0.55}\text{Li}_{0.35}\text{TiO}_3$  at low electrochemical potentials, thin layers of chemically stable PEO-salt complexes or ceramics such as LiPON have been placed between  $\text{La}_{0.55}\text{Li}_{0.35}\text{TiO}_3$  plates and lithium metal or lithiated graphite anodes.<sup>4,5</sup> The conductivities of these composite electrolytes can reach  $10^{-4} \text{ S-cm}^{-1}$ . However, their inflexibility and poor mechanical strength do not allow easy construction of suitable electrochemical secondary cells. Another possible design puts high-conductivity ceramic particles into a PEO-salt complex to form a composite solid polymer electrolyte.<sup>6</sup> However, poorly conducting interparticle contact results in little improvement in conductivity over that of PEO alone.

The approach suggested here to achieve high ionic conductivity combined with chemical and mechanical stability is the use of  $\text{La}_{0.55}\text{Li}_{0.35}\text{TiO}_3$  fibers and/or mats combined with PEO in which an additional very thin PEO layer is coated on the  $\text{La}_{0.55}\text{Li}_{0.35}\text{TiO}_3$  surface. A parallel approach, that of filling PEO with nonconducting ceramic (or glass) fibers and mats to reinforce polymer electrolytes, has been reported.<sup>7-9</sup> Incorporation of nonconducting ceramic fibers and mats into polymer electrolytes can enhance the mechanical properties of the electrolyte membranes, but decreases the ionic conductivity of the polymer electrolytes. However,  $\text{La}_{0.55}\text{Li}_{0.35}\text{TiO}_3$  fiber-PEO electrolytes not only have good mechanical strength but

also have high conductivity because the conducting fibers can penetrate the electrolyte film cross section to provide long-range Li<sup>+</sup> transfer channels. The conducting fibers in  $\text{La}_{0.55}\text{Li}_{0.35}\text{TiO}_3$  mat-PEO electrolytes have a similar function, but their woven pattern provides better bridging.

### Experimental

**Electrolyte preparation.**—PEO polymer (Aldrich; Mw 600,000 Da) was dried under vacuum at  $50^\circ\text{C}$  for 24 h. Lithium bis(perfluoroethylsulfonyl) imide [ $\text{LiN}(\text{SO}_2\text{CF}_2\text{CF}_3)_2$ ; 3M Company] and  $\text{LiClO}_4$  (Aldrich) were dried at  $120^\circ\text{C}$  for 24 h.  $\text{La}_{0.55}\text{Li}_{0.35}\text{TiO}_3$  ( $9.1 \times 10^{-4} \text{ S-cm}^{-1}$ ) particles less than  $1 \mu\text{m}$  were prepared from  $\text{Li}_2\text{CO}_3$ ,  $\text{La}_2\text{O}_3$ , and  $\text{TiO}_2$  starting materials using Inaguma's solid-state reaction method.<sup>1</sup> Stoichiometric amounts of these powders were ground together in an agate mortar and calcined at  $800^\circ\text{C}$  for 4 h to eliminate  $\text{CO}_2$ . The heated powder was ballmilled with ethanol for 1 day, and heated again at  $800^\circ\text{C}$  for 2 h. The ballmilled powder was then sieved through a #325 mesh for fiber and mat preparation.  $\text{La}_{0.55}\text{Li}_{0.35}\text{TiO}_3$  powders for filling PEO-LiClO<sub>4</sub> electrolytes were sintered at  $1325^\circ\text{C}$  for 2 h. The crystalline phases of  $\text{La}_{0.55}\text{Li}_{0.35}\text{TiO}_3$  powders were identified by X-ray diffraction (XRD) analysis at room temperature using Cu K $\alpha$  radiation. The  $2\theta$  range analyzed was  $10$ - $90^\circ$ , and the scan rate was  $2.0^\circ$  per second. The particle size was observed by scanning electron microscopy (SEM) images using a Jeol JSM-6400 microscope equipped with a Noran 1-2 energy-dispersive spectrometer. A 15 kV beam was employed to generate the backscattered-electron images. Sintered  $\text{La}_{0.55}\text{Li}_{0.35}\text{TiO}_3$  fibers of two different diameters (15 and 250  $\mu\text{m}$ ) were produced by Advanced Cerametrics, Inc. using its Viscous Suspension Spinning Process (VSSP) method.<sup>10</sup> In the VSSP method,  $\text{La}_{0.55}\text{Li}_{0.35}\text{TiO}_3$  powders were first dispersed in water to give a slurry, which was then mixed with viscose, *i.e.*, cellulose in aqueous sodium hydroxide solution. The mixture was then pumped through spinneret holes into a low-concentration sulfuric acid bath to form particulate  $\text{La}_{0.55}\text{Li}_{0.35}\text{TiO}_3$ -loaded cellulose (rayon) fibers. This was followed by sintering at  $1325^\circ\text{C}$  for 2 h. To fabricate  $\text{La}_{0.55}\text{Li}_{0.35}\text{TiO}_3$  mats, cellulose fibers loaded with  $\text{La}_{0.55}\text{Li}_{0.35}\text{TiO}_3$  particles were first woven into cloth-like mats, then sintered at  $1350^\circ\text{C}$  for 2 h.

$\text{La}_{0.55}\text{Li}_{0.35}\text{TiO}_3$  fiber-PEO composite electrolytes were prepared from acetonitrile dispersions of weighed quantities of fiber, lithium salt, and PEO to give 12.5 wt % Li<sup>+</sup> in the PEO matrix. These were ultrasonically vibrated for 8.0 h, cast onto poly(tetrafluoroethylene) films, and dried in air for 24 h, then vacuum dried at  $25^\circ\text{C}$ , followed by  $80^\circ\text{C}$ , each for 24 h.  $\text{La}_{0.55}\text{Li}_{0.35}\text{TiO}_3$  mat-PEO composite electrolytes were prepared by dropping a fresh solution of PEO and

\* Electrochemical Society Active Member.

\*\* Electrochemical Society Student Member.

<sup>z</sup> E-mail: cswang@tntech.edu

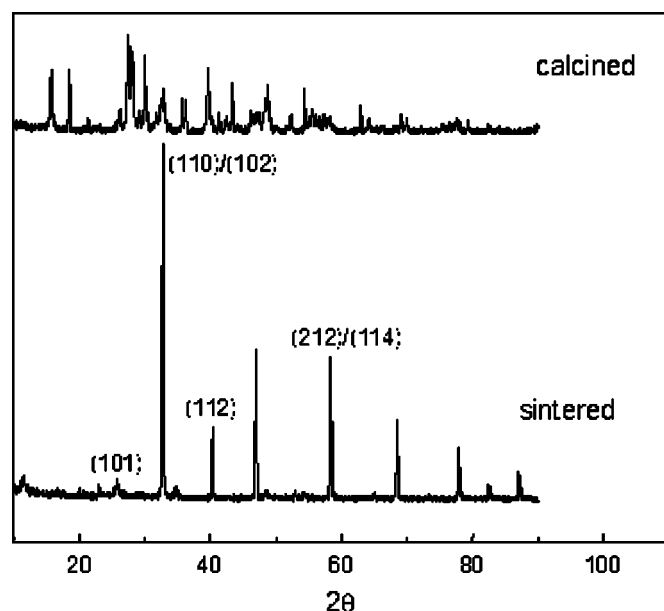


**Figure 1.** XRD patterns of  $\text{La}_{0.55}\text{Li}_{0.35}\text{TiO}_3$  powders calcined at  $800^\circ\text{C}$  and sintered at  $1325^\circ\text{C}$ .

lithium salt in the same wt % ratio dissolved in acetonitrile into  $\text{La}_{0.55}\text{Li}_{0.35}\text{TiO}_3$  mats, followed by rigorous drying as above.

**Electrochemical measurements.**—The ionic conductivity of the films was measured by electrochemical impedance spectroscopy (EIS) using symmetrical two-electrode cells sandwiching a film between two stainless steel plate electrodes. Spectra were obtained by sweeping from 65 kHz to 1 Hz with a Solartron FRA 1250 frequency analyzer and a Solartron model 1286 electrochemical interface. The high-frequency intercept of the Nyquist plot on the real axis gives the resistance  $R$  of the electrolyte, from which the ionic conductivity is calculated.  $\text{Li}^+$  transference number ( $t_{\text{Li}^+}$ ) measurements were conducted on symmetrical lithium/composite electrolyte/lithium cells by using the method of Bruce and Vincent.<sup>11</sup>

The stability of the composite electrolyte-lithium electrode interface was investigated by monitoring the time dependence of the impedance of symmetrical Li/composite electrolyte/Li cells under open-circuit conditions. This impedance measurement was obtained by sweeping from 65 kHz to 0.01 Hz using the same equipment as that for the ionic conductivity measurements.

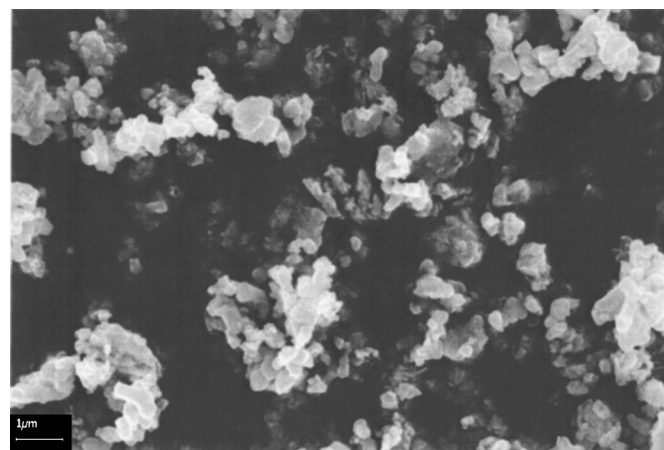


**Figure 2.** SEM images of the  $\text{La}_{0.55}\text{Li}_{0.35}\text{TiO}_3$  particles prepared by solid-state reaction.



**Figure 3.** A spool of green  $\text{La}_{0.55}\text{Li}_{0.35}\text{TiO}_3$  fiber of  $15\ \mu\text{m}$  diam.

## Results and Discussion

### Preparation of $\text{La}_{2/3-x}\text{Li}_x\text{TiO}_3$ particles, fibers, and mats.

Figure 1 shows the XRD patterns of  $\text{La}_{0.55}\text{Li}_{0.35}\text{TiO}_3$  powders calcined at  $800^\circ\text{C}$  and sintered at  $1325^\circ\text{C}$ . The powders calcined at  $800^\circ\text{C}$  consist only of a mixture of  $\text{La}_2\text{O}_3$ ,  $\text{Li}_2\text{O}$ , and  $\text{TiO}_2$ . However, the sintered powders were  $\text{La}_{0.55}\text{Li}_{0.35}\text{TiO}_3$ , which has a cubic perovskite-type structure. The XRD patterns of the sintered  $\text{La}_{0.55}\text{Li}_{0.35}\text{TiO}_3$  powders are in agreement with the previously reported XRD data of a ceramic with a similar composition.<sup>12</sup>  $\text{La}_{0.55}\text{Li}_{0.35}\text{TiO}_3$  powder disks were cold-pressed and sintered at  $1325^\circ\text{C}$  for 2 h. Their conductivity determined by EIS was *ca.*  $9.1 \times 10^{-4}\ \text{S}\cdot\text{cm}^{-1}$  at room temperature.

$\text{La}_{0.55}\text{Li}_{0.35}\text{TiO}_3$  fibers and mats were made from ballmilled  $\text{La}_{0.55}\text{Li}_{0.35}\text{TiO}_3$  particles using the VSSP method. Figure 2 shows SEM images of the ballmilled  $\text{La}_{0.55}\text{Li}_{0.35}\text{TiO}_3$  particles used to prepare fibers and mats. The particle size of  $\text{La}_{0.55}\text{Li}_{0.35}\text{TiO}_3$  was less than  $1\ \mu\text{m}$  after ballmilling for 1 day. Some  $\text{La}_{0.55}\text{Li}_{0.35}\text{TiO}_3$  particles were agglomerated to form large porous particles of 2–3  $\mu\text{m}$  diam.  $\text{La}_{0.55}\text{Li}_{0.35}\text{TiO}_3$ -loaded cellulose fibers (green fibers) of 15 and 250  $\mu\text{m}$  diam were successfully made from ballmilled  $\text{La}_{0.55}\text{Li}_{0.35}\text{TiO}_3$  particles. Figure 3 shows a spool of green  $\text{La}_{0.55}\text{Li}_{0.35}\text{TiO}_3$  fiber of  $15\ \mu\text{m}$  diam, which was woven into a mat (Fig. 4), then sintered at  $1325^\circ\text{C}$  for 2 h. Figure 5 shows sintered  $\text{La}_{0.55}\text{Li}_{0.35}\text{TiO}_3$  15  $\mu\text{m}$  diam fibers and sintered woven  $\text{La}_{0.55}\text{Li}_{0.35}\text{TiO}_3$  mats.

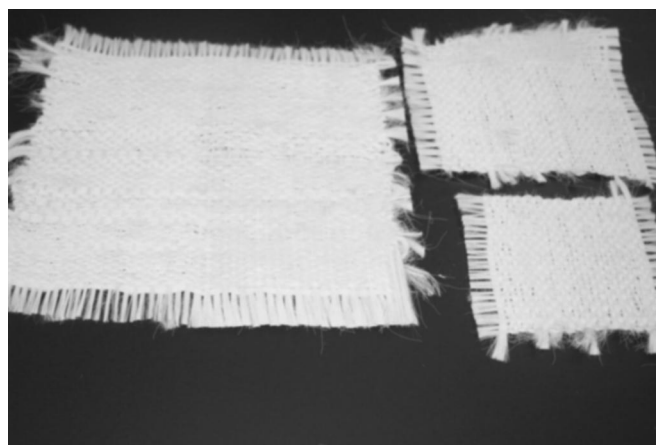


**Figure 4.** Woven mats made from green  $\text{La}_{0.55}\text{Li}_{0.35}\text{TiO}_3$  fibers of  $15\ \mu\text{m}$  diam.

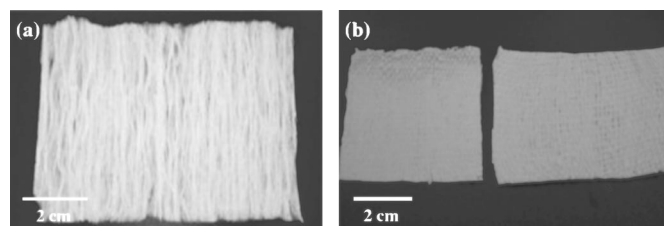


Figure 5. Sintered  $\text{La}_{0.55}\text{Li}_{0.35}\text{TiO}_3$  (a) fibers and (b) mats.

**Ionic conductivity of fiber-PEO electrolytes.**—Perovskite oxides of  $\text{ABO}_3$  type such as  $\text{La}_{0.67-x}\text{Li}_{3x}\text{TiO}_3$  have exceptional ionic conductivity, first reported by Inaguma.<sup>1</sup> However, ceramic membranes formed from these materials are brittle, making them difficult to use in secondary cells. The easiest way to give these materials flexibility is to load particles of ceramic into PEO-salt complexes to form composite polymer electrolytes, which have higher conductivity than the host PEO electrolytes.<sup>6</sup> In these conducting particle-PEO composite electrolytes, ceramic particles are homogeneously dispersed in the PEO matrix, and hence are separated by relatively thick polymer layers. The poorly conducting contacts between ceramic particles prevent much improvement of conductivity over that of the PEO host. However, conducting ceramic fibers can bridge the gap in the electrolyte film cross section, and hence provide long-range  $\text{Li}^+$  transfer channels. Figure 6 compares the ionic conductivities of electrolytes with 20 wt %  $\text{La}_{0.55}\text{Li}_{0.35}\text{TiO}_3$  particles and 20 wt %  $\text{La}_{0.55}\text{Li}_{0.35}\text{TiO}_3$  250  $\mu\text{m}$  diam fibers in  $\text{PEO-LiN}(\text{SO}_2\text{CF}_2\text{CF}_3)_2$ . The fiber-PEO electrolyte has higher conductivity than the particle-PEO electrolyte over the temperature range studied. The room-temperature conductivity of 20 wt %  $\text{La}_{0.55}\text{Li}_{0.35}\text{TiO}_3$  fiber-PEO- $\text{LiN}(\text{SO}_2\text{CF}_2\text{CF}_3)_2$  electrolyte was  $5.0 \times 10^{-4} \text{ S}\cdot\text{cm}^{-1}$ .

Figure 7 shows the temperature dependence of ionic conductivity for 50 wt %  $\text{La}_{0.55}\text{Li}_{0.35}\text{TiO}_3$  fiber-PEO- $\text{LiClO}_4$  electrolytes with different fiber diameters. Compared to thick fiber-PEO electrolytes, those with thin fibers have a higher area-to-volume ratio in the electrolyte film, giving higher conductivity over the whole temperature range. Fiber diameter therefore plays an important role in determining the ionic conductivity of fiber-PEO composite electrolytes, as does the choice of lithium salt. Figure 8 shows the temperature dependence of ionic conductivity for 250  $\mu\text{m}$  diam  $\text{La}_{0.55}\text{Li}_{0.35}\text{TiO}_3$  fiber-PEO- $\text{LiClO}_4$  and -PEO- $\text{LiN}(\text{SO}_2\text{CF}_2\text{CF}_3)_2$  electrolytes. Because the conductivity of  $\text{La}_{0.55}\text{Li}_{0.35}\text{TiO}_3$  fiber is not influenced by the presence of the lithium salt, any changes in electrolyte conductivity must occur in the PEO matrix.  $\text{LiN}(\text{SO}_2\text{CF}_2\text{CF}_3)_2$  has large anions which can influence the PEO polymer chain crystallization

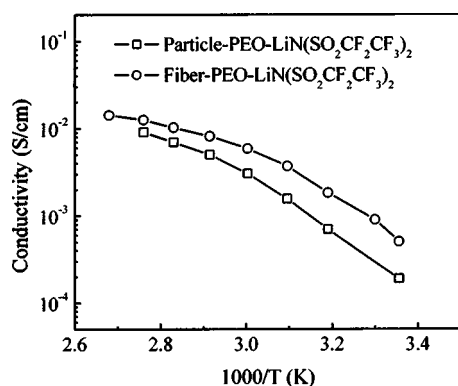


Figure 6. Arrhenius plots for the ionic conductivity of 20 wt %  $\text{La}_{0.55}\text{Li}_{0.35}\text{TiO}_3$  particle-PEO- $\text{LiN}(\text{SO}_2\text{CF}_2\text{CF}_3)_2$  and 20 wt % 250  $\mu\text{m}$  diameter  $\text{La}_{0.55}\text{Li}_{0.35}\text{TiO}_3$  fiber-PEO- $\text{LiN}(\text{SO}_2\text{CF}_2\text{CF}_3)_2$  composite electrolytes.

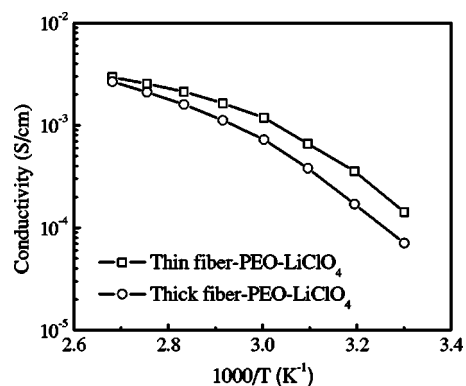


Figure 7. Arrhenius plots for the ionic conductivity of 50 wt %  $\text{La}_{0.55}\text{Li}_{0.35}\text{TiO}_3$  fiber-PEO- $\text{LiClO}_4$  composite electrolytes with differing fiber diameters. Thin fiber: 15  $\mu\text{m}$ , thick fiber: 250  $\mu\text{m}$ .

process, promoting amorphous regions with increased ionic conductivity. Therefore, the PEO matrix conductivity still plays an important role in the overall conductivity properties of these composite electrolytes, although the conducting fibers dominate in  $\text{Li}^+$  transfer.

One disadvantage of PEO-based polymer electrolytes is that polymer chain thermal motion can cause the amorphous PEO phase to slowly recrystallize at room temperature, which results in a loss of ionic conductivity during storage. Figure 9 shows the change in the relative conductivity ( $\sigma/\sigma_0$ ) for PEO- $\text{LiN}(\text{SO}_2\text{CF}_2\text{CF}_3)_2$  and 20 wt %  $\text{La}_{0.55}\text{Li}_{0.35}\text{TiO}_3$  fiber (250  $\mu\text{m}$ )-PEO- $\text{LiN}(\text{SO}_2\text{CF}_2\text{CF}_3)_2$  electrolytes over a 35 day period at 25°C. The conductivity of  $\text{La}_{0.55}\text{Li}_{0.35}\text{TiO}_3$  fiber, which penetrates the electrolyte cross section, does not change much during storage. At the same time, the ceramic fibers can also stabilize the conductivity of the PEO matrix by hindering its recrystallization. Therefore, the conductivity loss of  $\text{La}_{0.55}\text{Li}_{0.35}\text{TiO}_3$  fiber-PEO composite electrolyte is less than that of the host polymer electrolyte.

**Ionic conductivity and  $\text{Li}^+$  transference number of mat-PEO electrolytes.**—Fiber-PEO composite electrolytes have a higher conductivity than particle-PEO electrolytes because  $\text{La}_{0.55}\text{Li}_{0.35}\text{TiO}_3$  fibers can provide long-range  $\text{Li}^+$  transfer channels through the electrolyte film. However, most fibers are parallel to the film plane; hence, only some of the fibers can penetrate the electrolyte completely. Therefore, PEO host conductivity still plays an important role in the overall conductivity of fiber-PEO composite electrolytes, as is shown in Fig. 8. However, when the conducting fibers are woven into mats, they can penetrate the film cross section more readily. Figure 10 compares the ionic conductivities of 50 wt %

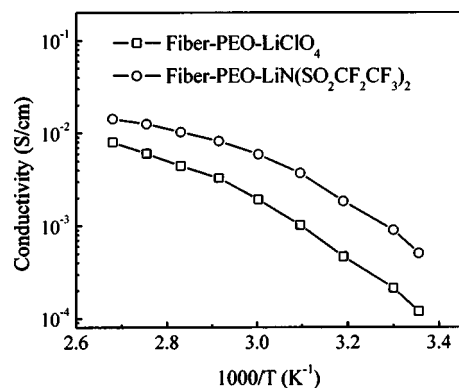
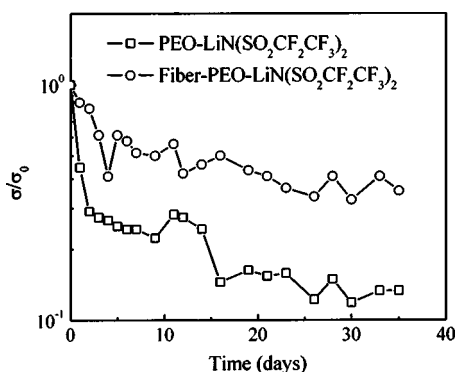


Figure 8. Arrhenius plots for the ionic conductivity of 20 wt %  $\text{La}_{0.55}\text{Li}_{0.35}\text{TiO}_3$  250  $\mu\text{m}$  diam fiber-PEO- $\text{LiClO}_4$  and PEO- $\text{LiN}(\text{SO}_2\text{CF}_2\text{CF}_3)_2$  composite electrolytes.



**Figure 9.** Relative conductivity ( $\sigma/\sigma_0$ ) vs. time for PEO-LiN(SO<sub>2</sub>CF<sub>2</sub>CF<sub>3</sub>)<sub>2</sub> and 20 wt % 250  $\mu\text{m}$  diameter La<sub>0.55</sub>Li<sub>0.35</sub>TiO<sub>3</sub> fiber-PEO-LiN(SO<sub>2</sub>CF<sub>2</sub>CF<sub>3</sub>)<sub>2</sub> composite electrolytes.

La<sub>0.55</sub>Li<sub>0.35</sub>TiO<sub>3</sub> fiber-PEO-LiClO<sub>4</sub> and 70 wt % La<sub>0.55</sub>Li<sub>0.35</sub>TiO<sub>3</sub> mat-PEO-LiClO<sub>4</sub> composite electrolytes. Fiber-PEO composite electrolytes with higher than 50 wt % fiber content are easily torn because the fibers are in parallel and the PEO matrix is not strong enough for bonding. The fiber content (70 wt %) of La<sub>0.55</sub>Li<sub>0.35</sub>TiO<sub>3</sub> mat-PEO-LiClO<sub>4</sub> electrolytes was obtained by weighing the La<sub>0.55</sub>Li<sub>0.35</sub>TiO<sub>3</sub> mat and PEO-LiClO<sub>4</sub> used. From Fig. 10, it is clearly seen that the mat-PEO composite electrolyte has higher conductivity than the fiber-PEO electrolyte over the whole temperature range studied because of its higher fiber content combined with its regular weave pattern.

The addition of conducting particles only slightly improves the Li<sup>+</sup> transference number.<sup>6</sup> However, the Li<sup>+</sup> transference number of La<sub>0.55</sub>Li<sub>0.35</sub>TiO<sub>3</sub> mat-PEO-LiClO<sub>4</sub> composite electrolyte was determined to be about 0.7, much higher than the highest number ( $t_{\text{Li}^+} = 0.39$ ) given by La<sub>0.55</sub>Li<sub>0.35</sub>TiO<sub>3</sub> particle-filled PEO electrolytes.<sup>6</sup> The high Li<sup>+</sup> transference number for the La<sub>0.55</sub>Li<sub>0.35</sub>TiO<sub>3</sub> mat-PEO-LiClO<sub>4</sub> composite electrolyte was attributed to the large amount of Li<sup>+</sup>-conducting ( $t_{\text{Li}^+} = 1.0$ ) La<sub>0.55</sub>Li<sub>0.35</sub>TiO<sub>3</sub> mat in the composite electrolytes.

**Interfacial stability with lithium electrode.**—La<sub>0.55</sub>Li<sub>0.35</sub>TiO<sub>3</sub> ceramic reacts with lithium metal, reducing the tetravalent titanium ions, and producing an electronic or electronic-ionic mixed conductor.<sup>1</sup> As a result, it is very important to prevent the direct contact of ceramic and lithium anodes. In fiber-PEO and mat-PEO composite electrolytes, the conducting ceramic is coated with a very thin PEO-salt layer, which separates the ceramic and lithium electrode. A 20 wt % La<sub>0.55</sub>Li<sub>0.35</sub>TiO<sub>3</sub> fiber-PEO-LiN(SO<sub>2</sub>CF<sub>2</sub>CF<sub>3</sub>)<sub>2</sub> was

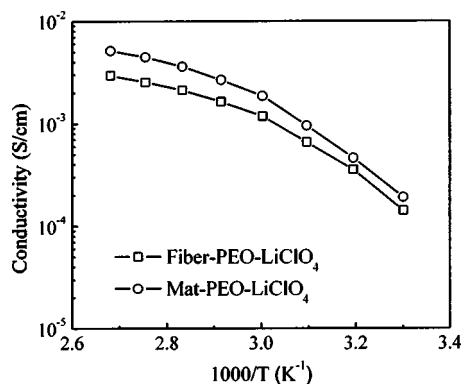


**Figure 10.** Arrhenius plots for ionic conductivities of 50 wt % La<sub>0.55</sub>Li<sub>0.35</sub>TiO<sub>3</sub> fiber-PEO-LiClO<sub>4</sub> and 70 wt % La<sub>0.55</sub>Li<sub>0.35</sub>TiO<sub>3</sub> mat-PEO-LiClO<sub>4</sub> composite electrolytes.

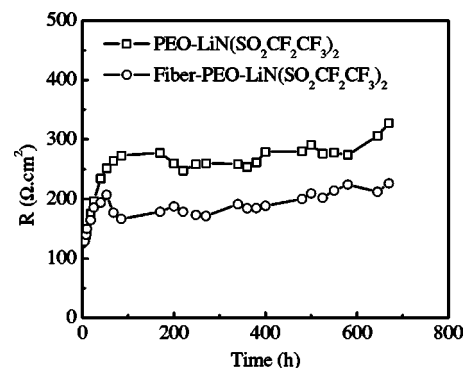


**Figure 11.** Interfacial resistances as a function of time for PEO-LiN(SO<sub>2</sub>CF<sub>2</sub>CF<sub>3</sub>)<sub>2</sub> and 20 wt % 250  $\mu\text{m}$  diam La<sub>0.55</sub>Li<sub>0.35</sub>TiO<sub>3</sub> fiber-PEO-LiN(SO<sub>2</sub>CF<sub>2</sub>CF<sub>3</sub>)<sub>2</sub> polymer electrolytes.

sandwiched between two lithium electrodes in a glove box. The color of the sample did not change with time, indicating that no reaction between La<sub>0.55</sub>Li<sub>0.35</sub>TiO<sub>3</sub> ceramic and lithium metal occurred, because the color changes from ivory to blue-black on reduction.<sup>1</sup>

Any reduction of tetravalent titanium ions starts at the electrolyte-electrode interface. The interfacial resistance between 20 wt % La<sub>0.55</sub>Li<sub>0.35</sub>TiO<sub>3</sub> fiber-PEO-LiN(SO<sub>2</sub>CF<sub>2</sub>CF<sub>3</sub>)<sub>2</sub> composite electrolyte and lithium electrode was monitored as a function of time, as shown in Fig. 11. The time dependence of the interfacial resistance for PEO-LiN(SO<sub>2</sub>CF<sub>2</sub>CF<sub>3</sub>)<sub>2</sub> polymer electrolyte is also shown. The interfacial resistance of the latter electrolyte increases markedly at first, then increases irregularly. The initial increase indicates formation of a passivation layer, and the subsequent irregular increase shows that its structure is unstable. The addition of La<sub>0.55</sub>Li<sub>0.35</sub>TiO<sub>3</sub> fiber should make the interfacial resistance more unstable if reaction is occurring. However, Fig. 11 shows that La<sub>0.55</sub>Li<sub>0.35</sub>TiO<sub>3</sub> fiber stabilizes the interfacial resistance, indicating no interfacial reaction. This interfacial stabilization is attributed to the ability of the La<sub>0.55</sub>Li<sub>0.35</sub>TiO<sub>3</sub> fiber surface to scavenge traces of residual impurities in a similar way to added nonconducting ceramic particles.<sup>13,14</sup>

## Conclusions

High-ionic-conducting La<sub>0.55</sub>Li<sub>0.35</sub>TiO<sub>3</sub> fibers and mats were successfully prepared using the VSSP method. La<sub>0.55</sub>Li<sub>0.35</sub>TiO<sub>3</sub> fibers in fiber-PEO and mat-PEO composite electrolytes can penetrate the electrolyte film, and hence provide long-range Li<sup>+</sup> transfer channels. La<sub>0.55</sub>Li<sub>0.35</sub>TiO<sub>3</sub> mat-PEO composite electrolyte has higher conductivity than fiber-PEO electrolyte because of the woven pattern and higher fiber content. The fiber diameter and the salt type also play an important role in the overall conductivity properties of composite electrolytes.

The reaction between La<sub>0.55</sub>Li<sub>0.35</sub>TiO<sub>3</sub> ceramic and lithium anodes is also prevented by the thin PEO-salt layer on the fiber surface. Therefore, these composite electrolytes have good interfacial stability with lithium metal and lithium-ion anodes.

## Acknowledgments

We gratefully acknowledge NASA-Glenn Research Center, Cleveland OH, for support of this work under grant no. NAG3-2617.

Tennessee Technological University assisted in meeting the publication costs of this article.

## References

1. Y. Inaguma, C. Liqun, M. Itoh, T. Nakamura, T. Uchida, H. Ikuta, and M. Wakihara, *Solid State Commun.*, **86**, 689 (1993).
2. A. Varez, M. L. Sanjuan, M. A. Laguna, J. I. Pena, J. Sanz, and G. F. de la Fuente, *J. Mater. Chem.*, **11**, 125 (2001).

3. C. Wang, P. Patil, A. J. Appleby, F. E. Little, M. Kesmez, and D. L. Cocke, *J. Electrochem. Soc.*, **151**, A1196 (2004).
4. W. C. West, J. F. Whitacre, and J. R. Lim, *J. Power Sources*, **126**, 134 (2004).
5. Y. Kobayashi, H. Miyashiro, T. Takeuchi, H. Shigemura, N. Balakrishnan, M. Tabuchi, H. Kageyama, and T. Iwahori, *Solid State Ionics*, **152**, 137 (2002).
6. X. W. Zhang, C. Wang, A. J. Appleby, and F. E. Little, *J. Power Sources*, **112**, 209 (2002).
7. C. Yang and S. Lin, *J. Power Sources*, **112**, 497 (2002).
8. H. Park, J. Chun, S. Kim, J. Ko, S. Jo, J. Chung, and H. Sohn, *J. Power Sources*, **92**, 272 (2001).
9. Z. Wen, M. Wu, T. Itoh, M. Kubo, Z. Lin, and O. Yamamoto, *Solid State Ionics*, **148**, 185 (2002).
10. <http://www.advancedceramics.com/acitechnology.htm>
11. P. G. Bruce and C. A. Vincent, *J. Electroanal. Chem. Interfacial Electrochem.*, **225**, 1 (1977).
12. J. Ibarra, A. Varez, C. Leon, J. Santamaria, L. M. Torres-Martinez, and J. Sanz, *Solid State Ionics*, **134**, 219 (2000).
13. G. B. Appetecchi, F. Croce, L. Persi, F. Ronci, and B. Scrosati, *Electrochim. Acta*, **45**, 1481 (2000).
14. F. Croce, L. Persi, F. Ronci, and B. Scrosati, *Solid State Ionics*, **135**, 47 (2000).